

DIRECT-BIOGAS SOLID OXIDE FUEL CELL (SOFC) – A THEORETICAL ANALYSIS¹

Aline Lima da Silva²
Nestor Cezar Heck³

Abstract

The present work is aimed at analyzing the direct feeding of biogas to SOFC anodes. SOFCs are suitable for electricity generation from biogas, and it is possible to run SOFCs even on biogas compositions richer in CO₂ – under such conditions, conventional heat engines would not work, due to difficulty in maintaining ignition. By means of a thermodynamic analysis, it is possible to show that SOFCs can be operated on gas mixtures with CH₄/CO₂ molar ratios ranging from 0.1:1 (CO₂ rich mixture) to 2:1 (CH₄ rich mixture). The effect of operating temperature and current on the composition of the anode atmosphere, efficiency and carbon deposition is discussed. The influence of biogas contaminants – NH₃ and H₂S – on SOFC performance is evaluated. Under certain operating conditions, it is demonstrated that CeO₂ addition on Ni/YSZ can increase the resistance of the catalyst against sulfur poisoning by the H₂S. The effect of operating current on Ni poisoning by H₂S is also investigated.

Key words: H₂S; Biogas; SOFC; Thermodynamic simulation.

¹ Technical contribution presented at the 68th ABM International Congress, July 30st-Aug. 2nd 2013, Belo Horizonte, Brazil.

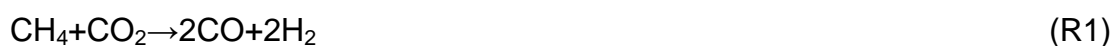
² Dr., Postdoctoral researcher, Núcleo de Termodinâmica Computacional para a Metalurgia, NTCm PPGE3M, UFRGS, Porto Alegre, RS, Brasil; adasilva26@gmail.com.

³ Metallurgical Engineer. Dr., Professor, Núcleo de Termodinâmica Computacional para a Metalurgia, NTCm; Depto. de Metalurgia, PPGE3M, UFRGS, Porto Alegre, RS, Brasil; heck@ufrgs.br.

1 INTRODUCTION

Biogas is a highly variable mixture of gases predominantly consisting of methane and carbon dioxide, besides other gases, including ammonia (NH₃) and H₂S.⁽¹⁾ One of the principal limitations of biogas is its variability of composition, not only in different locations but also over time, and often low level of methane which presents difficulties in its use in conventional power systems.⁽²⁾ According to Staniforth and Ormerod,⁽³⁾ as the proportion of CO₂ in the biogas increases, the fuel becomes progressively more difficult to ignite, and eventually the proportion of CO₂ becomes such that ignition can no longer be maintained. In practice, conventional heat engines are not operated at methane levels below 50%. Due to this limitation, large quantities of biogas are simply vented to atmosphere, wasting a potentially clean, renewable energy source.

The most attractive feature of SOFCs is their fuel flexibility due to the high operating temperature (973-1273K).⁽⁴⁾ Biogas can therefore be considered as a possible fuel source for the SOFC.⁽³⁾ It has been reported that SOFCs can generate considerable power even at 20% methane to carbon dioxide while the combustion engines cannot be applicable under this condition.⁽³⁾ Direct feeding of real biogas generated in a methane fermentation reactor to SOFC would represent an environmental-friendly, compact and cost-effective energy conversion system in which dry reforming of CH₄ (R1) proceeds on Ni-based anode using the CO₂ intrinsically contained in biogas, with no need of external reformer. The produced H₂ and CO are electrochemically oxidized to produce electricity (R2 and R3). For CH₄/CO₂ molar ratios >1, electrochemical oxidation of CH₄ occurs (R4).⁽⁵⁾



Direct feeding of biogas would be possible for high temperature SOFC, however, Ni/YSZ anode has a tendency toward carbon deposition and is deactivated drastically by H₂S poisoning.⁽⁵⁾

In the present work, the effect of operating temperature and current on the composition of the anode atmosphere and carbon deposition is discussed. By means of a thermodynamic analysis, it is shown that SOFCs can be operated on gas mixtures with CH₄/CO₂ molar ratios ranging from 0.1:1 (CO₂ rich mixture) to 2:1 (CH₄ rich mixture). The influence of biogas contaminants – NH₃ and H₂S – on SOFC performance is evaluated. Under certain operating conditions, it is demonstrated that CeO₂ addition on Ni/YSZ can increase the resistance of the catalyst against sulfur poisoning by the H₂S. The effect of operating current on Ni poisoning by H₂S is also investigated.

2 METHODOLOGY

Thermodynamic equilibrium calculations using the Gibbs energy minimization approach were carried out using the commercial software FactSage 6.3.

The selected databases were SGPS and FactPS, which include thermodynamic data for compounds only. The species considered for describing the ideal gas phase were: H₂, H₂O, H₂S, CO, CO₂, CH₄, O₂, S₂, COS, CS, CS₂, SO₂, SO₃, S₂O, NH₃, NO,

N₂O, NO₂, NO₃, N₂O₃, N₂O₄, N₂O₅. The solid phase graphite was considered in the compounds data set to predict carbon deposition over the catalyst. The solid phases selected to describe the Ce-O-S system were the following: CeO_{1.72}, CeO_{1.83}, CeO₂, Ce₂O₂S, Ce₂(SO₄)₃, CeS, Ce₃S₄, Ce₂S₃, Ce₂O₃. The solid phases selected to describe the Ni-S-O system were the following: Ni, Ni₃S₂, Ni₃S₄, Ni₆S₅, NiS, NiS₂, NiSO₄, NiO.

With respect to sulfur poisoning mechanism for Ni-based catalysts used in anodes of SOFCs (typically Ni-YSZ cermet anodes), it would be interesting to pause here and discuss it briefly based on the experimental results reported for electrochemical measurements in SOFCs. According to Ashrafi et al.,⁽⁶⁾ the poisoning of the nickel catalyst may occur even when the concentration of hydrogen sulfide ought not to cause the formation of a bulk nickel sulfide. Therefore, hydrogen sulfide may be assumed to be retained by a chemisorption process. The loss of activity of Ni-based catalysts through sulfur compounds could be due to strong sulfur chemisorption on the nickel surface, which prevents the further adsorption of reactant molecules. In a Ni-YSZ cermet anode, sulfur poisoning is characterized by a rapid initial drop in power output upon exposure to sulfur-containing fuels.⁽⁷⁾ For describing sulfur chemisorption, Rostrup-Nielsen Jr.⁽⁸⁾ used a Temkin-like isotherm:

$$\frac{pH_2S}{pH_2} = \exp\left(\frac{\Delta H_0^0(1-\alpha\theta)}{RT} - \frac{\Delta S_0^0}{R}\right) \quad (1)$$

Based on Equation 1, the equilibrium surface coverage (θ) will be calculated, in the present work, as:

$$\theta = \frac{\ln\left(\frac{pH_2S}{pH_2}\right) + \frac{\Delta H_0^0}{RT} + \frac{\Delta S_0^0}{R}}{\frac{\alpha\Delta H_0^0}{RT}} \quad (2)$$

With a ΔH_0^0 of 289 kJ mol⁻¹, a ΔS_0^0 of -19 J mol⁻¹ K⁻¹, and a α of 0.69.

After each equilibrium calculation carried out using the Gibbs energy minimization approach, the obtained pH₂S/pH₂ ratio is replaced in Equation 2, and the surface coverage value can be known. Operating conditions under which θ value can be diminished are determined in the present research. CeO₂ is added to the system to evaluate its beneficial effects on the reduction of θ value. The lower the Ni surface coverage, the lower the catalyst poisoning. Consequently, the drop in power output due to H₂S poisoning will be reduced.

Biogas inlet feed ratio considered in calculations is of 1.9L/h. Total mass of catalyst is assumed to be 0.83 g (85mol% Ni, 5mol% CeO₂, remaining YSZ; Ni/CeO₂ molar ratio of 20:1). In this way, it is supposed a space velocity of 2.3L/hg_{catalyst}, which can be reached during SOFC operation. In the section 3.3, ammonia feed ratio was also assumed to be 1.9 L/h. However, it is worth pointing out here that, for Figures 2 and 3 shown in the results section, different values of biogas inlet feed ratio were considered in order to compare with experimental results. Such values are indicated in figure captions.

When an SOFC is producing a current, there is a net input of oxygen ions (O²⁻) to the anodic compartment that changes the equilibrium conditions of the system. Thus, moles of oxygen (n_O) must be added to the system, as shown in Equation 3.

$$n_o \text{ (mol} \cdot \text{h}^{-1}\text{)} = \left(\frac{I}{2F}\right) \times 3600 \quad (3)$$

I is the current (A) and F is the Faraday constant (96485.34 C mol⁻¹).

The reversible electrical potential difference across the electrolyte of an SOFC is related to the difference in chemical potentials.⁽⁹⁾ The electrode reactions involving oxygen gas (O₂) at anode and cathode are, respectively:

- $2O^{2-} = O_2(p_{O_2}^{an.}) + 4e^-$
- $O_2(p_{O_2}^{cat.}) + 4e^- = 2O^{2-}$

Hence, the virtual cell reaction is:



Therefore, oxygen is transferred from a higher chemical potential (cathode) to a lower chemical potential (anode). The Gibbs free energy change for this cell reaction, ΔG_{R5} , is equal to the difference between the chemical potentials on opposite sides of the electrolyte:

$$\Delta G_{R5} = \mu_{O_2}^{an.} - \mu_{O_2}^{cat.} = RT \ln \left(\frac{p_{O_2}^{an.}}{p_{O_2}^{cat.}} \right) = -4FE \quad (4)$$

Thus, EMF (E) – electromotive force of a cell (V) for reversible conditions – is given by the following equation:

$$E = \frac{RT}{4F} \ln \frac{p_{O_2}^{cat.}}{p_{O_2}^{an.}} \quad (5)$$

In Equation 5, the value of $p_{O_2}^{cat.}$ is 0.21 atm, and $p_{O_2}^{an.}$ is known from the equilibrium calculation. When no current is drawn (unloaded SOFC), EMF is referred as OCV (open circuit voltage).

3 RESULTS AND DISCUSSION

3.1 Biogas Conversion in SOFC Anodes

Figure 1a depicts equilibrium composition for exit gas from an unloaded SOFC along with experimental values from Staniforth e Ormerod.⁽³⁾ Theoretical analysis shows that, as biogas becomes richer in CH₄, concentration of H₂ in biogas increases, while the concentration of CO₂ decreases continuously. With respect to CO, one can see that its concentration increases until reaching a maximum value, at ~47% methane in biogas. At higher contents of methane in biogas, solid carbon formation increases. These results suggest that dry reforming (R1) initially occurs and, when methane content in biogas is elevated (> 47%), methane decomposition takes place (R6). Thus, for methane content in biogas >47%, CO decreases while C(s) increases. Interestingly, as can be seen from Figure 1a, theoretical and experimental values for H₂ concentration agree until ~47% methane in biogas. At higher methane contents, experimental results show that the concentration of H₂ decreases. This discrepancy between theoretical and experimental values can be attributed to catalyst deactivation by carbon deposition, since theory predicts that the system is very prone

to form solid carbon. Theoretical and experimental values agree perfectly for CO₂ concentration over the whole range of methane content in biogas. The maximum CO content obtained in experiments coincides with theoretical value. Figure 1b shows that CH₄ in exhaust gas increases abruptly with methane content in biogas. In fact, this can be due to deactivation of catalyst. Theoretical analysis shows a concentration much lower than experimental values, although thermodynamics also indicates that CH₄ concentration in exhaust gas increases with methane content in biogas. Figure 1c shows that high OCV values can be reached with biogas compositions richer in CH₄, since more reducing condition (lower pO₂ and higher pH₂) are achieved when % methane in biogas is elevated (Figure 1d). Figure 2 shows the effect of methane content in biogas on the SOFC power. Results from thermodynamic analysis are compared with experimental results from Staniforth e Ormerod.⁽³⁾ Obviously, current values predicted from thermodynamic analysis for a SOFC operating at 0.7V are higher than the current measured by a potentiostat. Irreversible losses are not included. SOFC efficiency can be estimated by dividing the experimental by the theoretical power. Interestingly, even for a biogas composition poor in CH₄ (only 10%) a power of ~200mWatts can be attained, with an efficiency of 60%. As biogas becomes richer in CH₄, SOFC power increases, even though the efficiency decreases. For an inlet mixture containing 41.63% of methane, the efficiency is of ~25%. However, this decreasing trend of efficiency with methane content in biogas is not a rule, since the value of power experimentally obtained will depend on the characteristics (composition, microstructure, etc.) of the SOFC anode material.

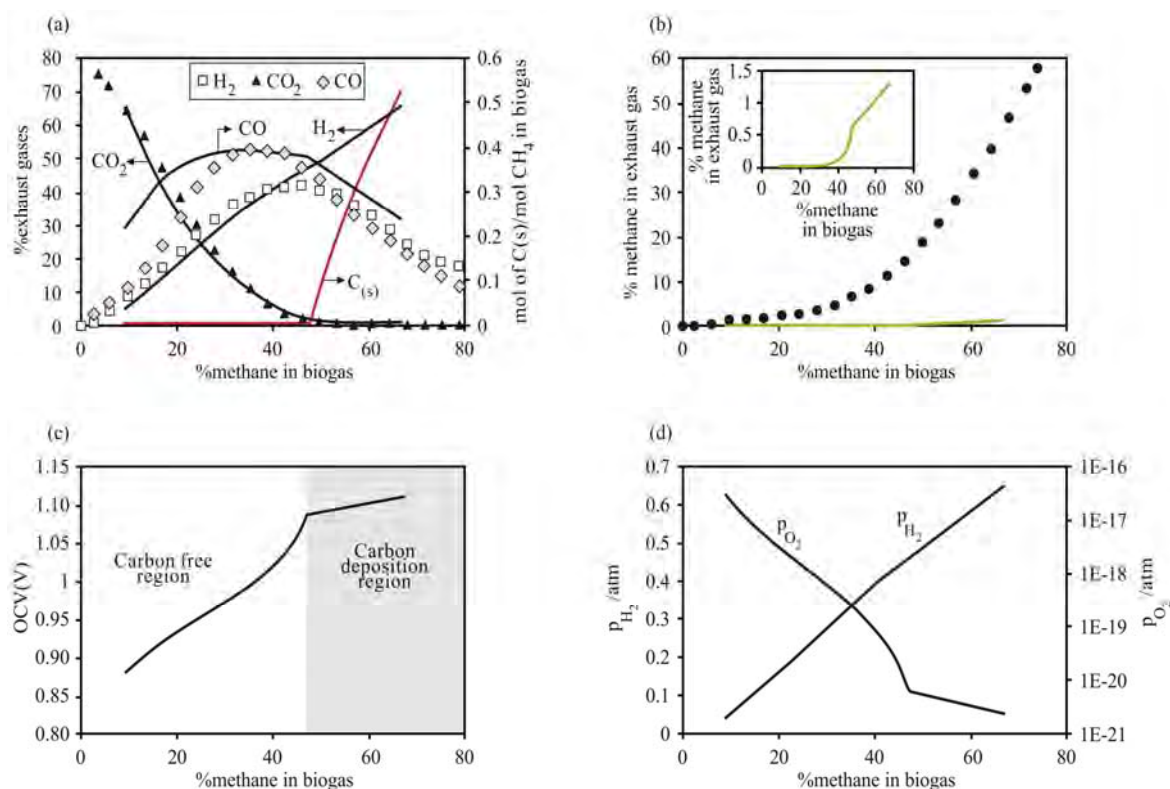


Figure 1. Effect of methane content in biogas on (a) exhaust gas composition (H₂, CO₂ and CO) and carbon deposition; (b) methane content in exhaust gas; (c) OCV; and (d) partial pressure of H₂ and O₂. Biogas flow rate = 6 ml/min, cell potential =0.7V. T=1.123K. Solid lines refer to theoretical values computed in the present work, and the markers are experimental values reported in Staniforth e Ormerod.⁽³⁾

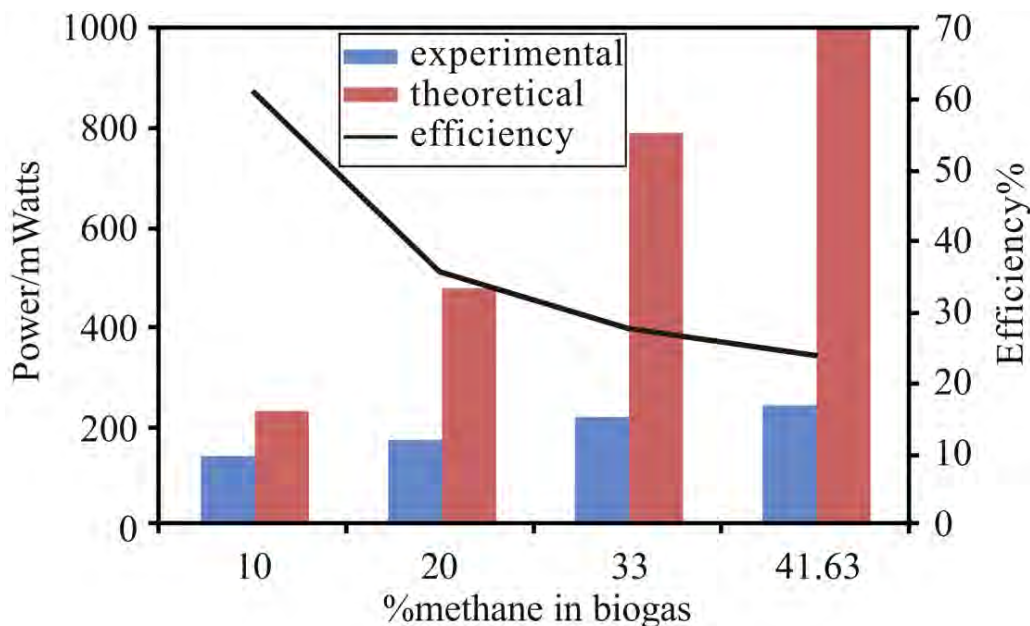


Figure 2. Effect of methane content in biogas on power and efficiency. Experimental values obtained from Staniforth e Ormerod.⁽³⁾ Biogas flow rate = 6 ml/min, cell potential =0.7V. T=1.123K.

Figure 3a shows the equilibrium of the main species (H_2 , CO , H_2O , CO_2 , CH_4) and EMF as a function of current for an SOFC operating on biogas (CH_4/CO_2 molar ratio=2:1). Carbon deposition region disappears with increased load. CO concentration increases within the carbon deposition region. It should be noted that within carbon deposition region H_2 concentration and E change slightly, while CH_4 exists at a constant concentration. Only after the carbon deposition region H_2O and CO_2 increase with significant consumption of H_2 , resulting in lower values of E . Figure 3b depicts theoretical and experimental values of SOFC power operating on biogas and the efficiency. At the maximum value of power obtained experimentally, the efficiency is of ~50%. Thus, SOFCs operating on CH_4 -rich biogas can achieve high efficiencies. Such performance will depend on optimization of anode material. While Figure 2 shows an efficiency of 25% for a methane rich biogas (41.63%), Figure 3b shows the possibility of achieving an efficiency of 50% for a biogas even richer in CH_4 (67%).

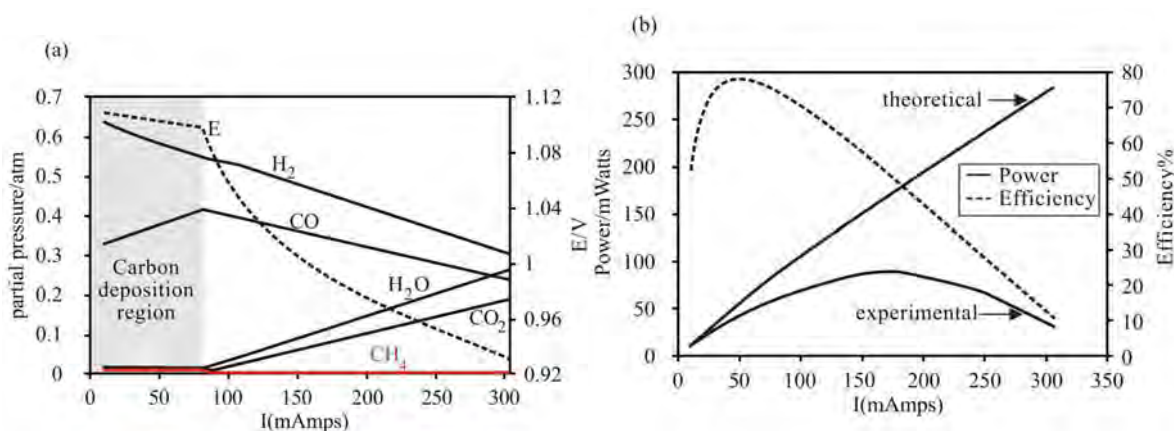


Figure 3. Effect of current on: (a) partial pressure (H_2 , CO , H_2O , CO_2 , CH_4), carbon deposition region and E ; (b) power and efficiency. T=1123K. Feedstock: $1\text{ cm}^3\text{ min}^{-1}\text{ CH}_4 + 0.5\text{ cm}^3\text{ min}^{-1}\text{ CO}_2$. Experimental results from Laycock, Staniforth e Ormerod.⁽¹⁾

3.2 Effect of CeO₂ Addition on Prevention of Ni Poisoning by H₂S During Biogas Conversion in SOFC Anodes

Figure 4 shows the effect of CeO₂ addition on Ni poisoning by H₂S. Figure 4a shows that within carbon deposition region Ce₂O₂S phase can be formed, lowering p_{H₂S}, which results in lower values of surface coverage (θ) of Ni catalyst when compared with a catalyst without addition of CeO₂ (Figure 4b). Within carbon deposition region, ceria assumes the reduced form (CeO_{1.71}). As current increases, ceria becomes more oxidized (CeO_{1.83}). The formation of H₂O and CO₂, with the lowering of partial pressure of H₂, is unfavorable for formation of Ce₂O₂S phase. Thus, there is a range of operating current at which CeO₂ can be effective in lowering θ values and, in this way, Ni poisoning. Even though CeO₂ can reduce θ values, it should be noted that Ni poisoning still occurs, since θ values fall in the region of diagram corresponding to chemisorption of S on Ni surface. However, the effects of Ni poisoning, e.g. reduction of SOFC power, will be lower in comparison with Ni catalyst without CeO₂ addition (Figure 4b). Clean Ni surface is observed only for θ values lower than 0.6 (such reference value was taken from diagram published in Wang e Liu⁽¹⁰⁾). Figure 4c shows the partial pressure of sulfur-containing species as a function of current. As can be seen, the partial pressure of H₂S is much higher than that of other species. SO₂ is, from a practical point of view, not formed (partial pressure in the range of 1E-14-1E-12atm). This is reasonable to expect, due to extremely reducing anode atmosphere (p_{O₂} in the range of 1E-20-1E-18atm).

3.3 Ammonia Conversion in SOFC Anodes

Ammonia is a biogas contaminant. Typically, NH₃ is present at 100 ppm in biogas.⁽¹¹⁾ In this way, it is important to verify if SOFCs are tolerant to NH₃ and if it is possible to produce electricity from NH₃ with no formation of any undesirable nitrogen oxides. Figure 5a shows that, at 673K, NH₃ is totally converted into N₂ and H₂. Thus, at SOFC operating temperature, e.g. 1.123K, NH₃ is decomposed in N₂ and H₂. Figure 5b shows that, as current is drawn from the cell, H₂ is electrochemically oxidized to H₂O, while partial pressure of N₂ remains constant. In this way, NH₃ can be seen as fuel, not as contaminant. Figure 5c shows the partial pressure of nitrogen oxides as a function of current. From a practical point of view, nitrogen oxides are not formed during SOFC operation. This is reasonable to expect, due to extremely reducing anode atmosphere (p_{O₂} in the range of 1E-24-1E-17atm). Experimental reports for NH₃ utilization in SOFCs are in excellent agreement with theoretical findings of this work.

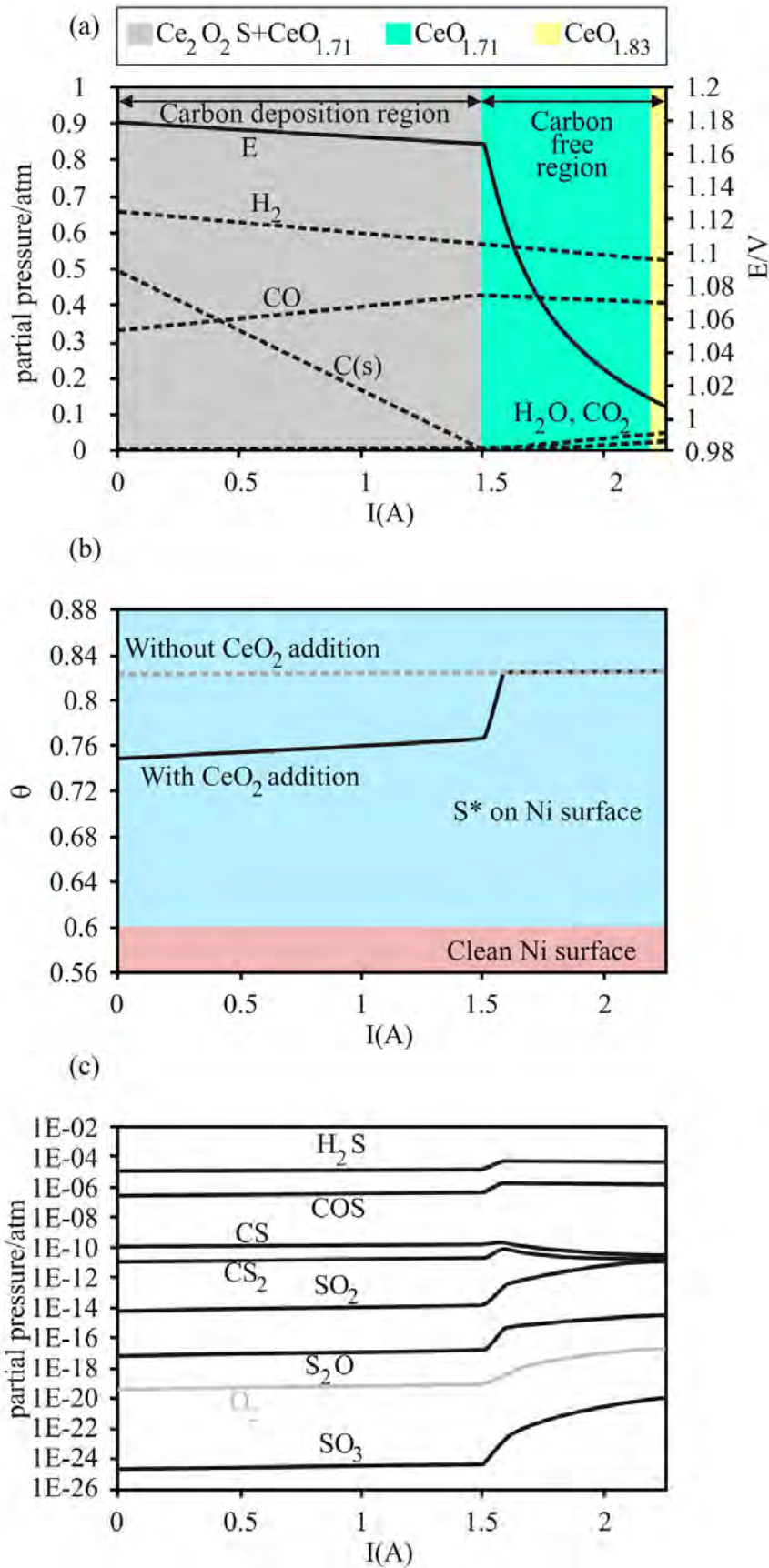


Figure 4. Effect of current on (a) Phase equilibria of Ce-O-S system, carbon deposition region, E and partial pressure of each species in the gas phase; (b) θ values; and (c) partial pressure of sulfur-containing species and O_2 . H_2S content=100 ppm; $T=1.273K$.

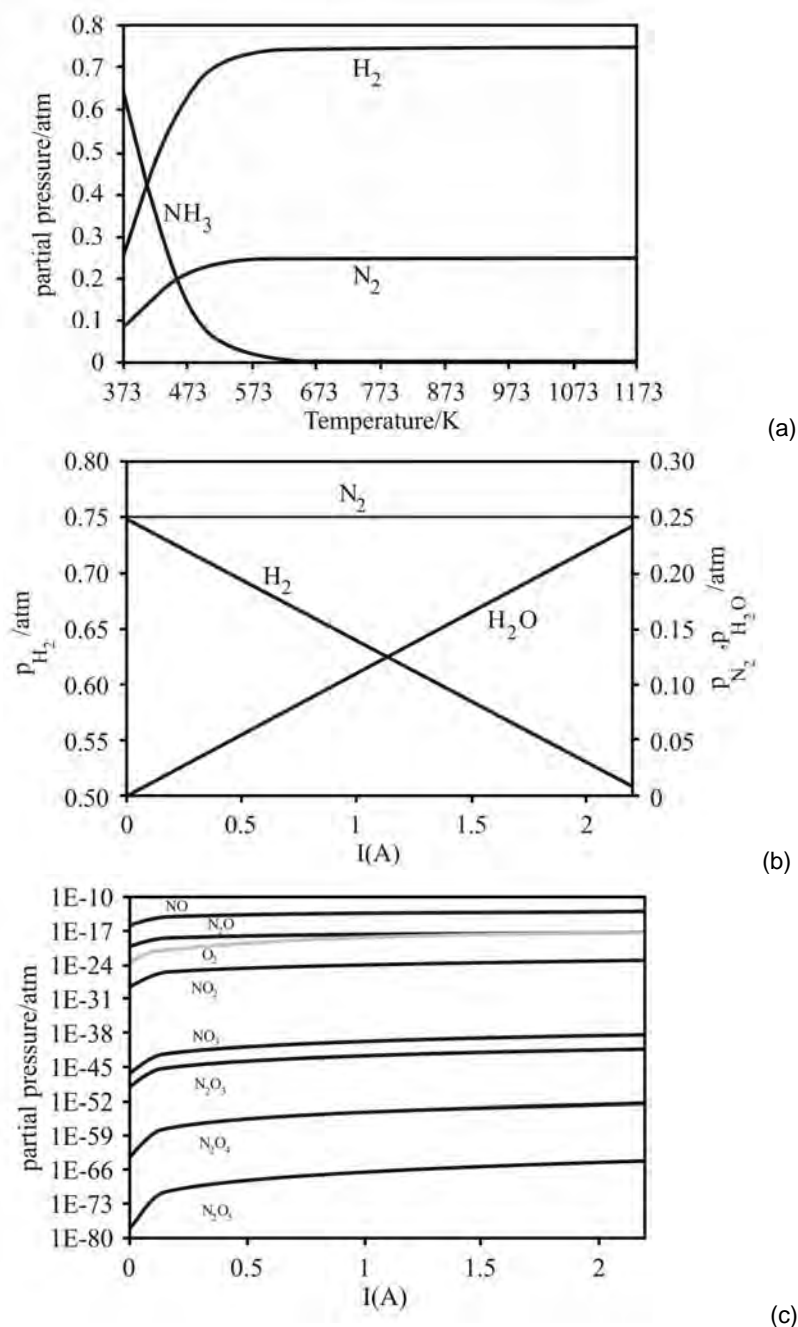


Figure 5. (a) Partial pressure of NH_3 , N_2 and H_2 as a function of temperature; partial pressure, as a function of current, of; (b) N_2 , H_2 and H_2O ; and (c) nitrogen oxides, O_2 . $T=1123\text{K}$ for (b) and (c).

4 CONCLUSIONS

The present work was aimed at analyzing the direct feeding of biogas to SOFC anodes. The following conclusions can be drawn from the present study:

- it is theoretically demonstrated that SOFCs can run directly on biogas over a wide compositional range of methane. The results are experimentally validated. The electrical power varies with methane content of the biogas. The higher methane content in biogas, the higher the power. Methane is reformed by CO_2 producing H_2 and CO , which are electrochemically oxidized. High contents of methane result in significant carbon deposition, due to methane decomposition, forming graphite and H_2 . Solid carbon can be gasified as

current increases. At maximum power, an efficiency of 50% is achieved, as can be verified from experimental reports and theoretical results;

- under certain operating conditions, it is demonstrated that CeO₂ addition on Ni/YSZ can increase the resistance of the catalyst against sulfur poisoning by the H₂S. There is a range of operating current at which CeO₂ can be effective in lowering θ values and, in this way, Ni poisoning. Ceria becomes more oxidized as current increases. Sulfur oxides are not stable even when current is drawn from SOFCs;
- ammonia can be seen as a fuel. NH₃ is decomposed to N₂ and H₂, with subsequent electrochemical oxidation of H₂. Nitrogen oxides are not stable during SOFC operation.

Acknowledgments

The authors would like to thank FAPERGS (Fundação de Amparo à Pesquisa do Estado do Rio Grande do Sul) and CAPES (Coordenação de Aperfeiçoamento de Pessoal de Nível Superior) for their financial support (Postdoctoral fellowship – Edital 09/2012 - DOCFIX).

REFERENCES

- 1 Laycock CJ, Staniforth JZ, Ormerod RM. Biogas as a fuel for solid oxide fuel cells and synthesis gas production: effects of ceria-doping and hydrogen sulfide on the performance of nickel-based anode materials. *Dalton Transactions* 2011;40: 5494–5504.
- 2 Huang J, Crookes RJ. Assessment of simulated biogas as a fuel for the spark ignition engine. *Fuel* 1998; 77: 1793-1801.
- 3 Staniforth J, Ormerod RM. Running Solid oxide Fuel Cells on Biogas. *Ionics* 2003; 9: 336- 341.
- 4 Steele BCH, Heinzl A. Materials for fuel-cell technologies. *Nature* 2001; 414:345-352.
- 5 Shiratori Y, Oshima T, Sasaki K. Feasibility of direct-biogas SOFC. *Int J Hydrogen Energy* 2008; 33: 6316-6321.
- 6 Ashrafi M, Pfeifer C, Pröll T, Hofbauer H. Experimental Study of Model Biogas Catalytic Steam Reforming: 2. Impact of Sulfur on the Deactivation and Regeneration of Ni-Based Catalysts. *Energy & Fuels* 2008; 22: 4190-4195.
- 7 Cheng Z, Wang JH, Choi YM, Yang L, Lin MC, Liu M. From Ni-YSZ to sulfur-tolerant anode materials for SOFCs: electrochemical behavior, in situ characterization, modeling, and future perspectives. *Energy & Environmental Science* 2011; 4: 4380-4409.
- 8 Rostrup-Nielsen JR. High temperature hydrogen sulfide chemisorption on nickel catalysts. *Appl Catal* 1981; 1: 303-314.
- 9 Rao YK. Stoichiometry and thermodynamics of metallurgical processes. Cambridge: Cambridge University Press; 1985.
- 10 Wang JH, Liu M. Computational study of sulfur–nickel interactions: A new S–Ni phase diagram. *Electrochemistry communications* 2007; 9: 2212-2217.
- 11 Kolbitsch P, Pfeifer C, Hofbauer H. Catalytic steam reforming of model biogas. *Fuel* 2008; 6: 701-706.